Proceedings of The National Conference
On Undergraduate Research (NCUR) 2020
Montana State University, Bozeman MT
March 26-28, 2020

Effect of Quinoline Amide Substituents on the Luminescence Properties of Bimodal Europium (III) Complexes

Brooke Aloe, Marisa Poveda
Department of Chemistry
University of San Francisco
San Francisco, California

Faculty Advisor: Dr. Osasere Evbuomwan

Abstract

The use of traditional optical imaging probes such as fluorescent, organic molecules and proteins *in vivo* is limited by phenomena such as autofluorescence and photobleaching. This limitation makes differentiating signal due to naturally luminescent biological molecules and the luminescent probe of interest extremely difficult. Lanthanide ions such as Eu(III) are known to exhibit long luminescence lifetimes, allowing for time-resolved luminescent image acquisition; however, the use of high energy lasers to directly excite these ions could potentially be damaging to biological tissue. To address this issue, organic chromophores such as quinolines can be used to absorb the incident light and transfer it to a nearby lanthanide ion. This intramolecular energy transfer results in the indirect sensitization of the lanthanide ion luminescence. Although quinoline antennas exhibit triplet state energies similar to that of europium (III) ions, efficient sensitization is reliant on the proximity of the antenna to the lanthanide ion. The goal of this project is to investigate the effect of different quinoline amide substituents on the optical imaging and MRI properties of bimodal europium (III) complexes. To date, a library of europium (III) complexes comprised of an octadentate chelating ligand with an appended quinoline antenna has been synthesized. Upon spectroscopic analysis of these complexes, indirect sensitization of the europium (III) luminescence by the quinoline pendant arm was observed for all complexes in the library, the magnitude of which was found to be dependent on the position of the amide substituent. Using phosphorescence lifetime measurements in D_2O and H_2O, the majority of complexes have been estimated to possess one bound water molecule, which is necessary for MR agents to produce a contrast signal. Future work will include evaluation of the MRI properties of these complexes to better understand the effect of the different quinoline substituents on water exchange rates.

Keywords: Optical Imaging Agents, Europium(III) Complexes, Quinoline Antenna Sensitization

1. Introduction

Surgical intervention is often used in the management of cancers; however the discrimination between malignant and healthy tissue is a major obstacle that can either lead to insufficient resection of cancerous tissue, or excision of considerable amounts of healthy tissue. The use of a dual-modality imaging agent with both Magnetic Resonance Imaging (MRI) and Optical Imaging properties could potentially improve tumor visualization before and during surgery.[1,2] The administration of such an agent would provide preoperative MR images to localize the bulk of the tumor, and intraoperative fluorescence imaging to elucidate tumor margins below the MRI detection limit. This approach, referred to as "targeted surgery," has the potential to reduce the need for multiple surgeries, thus improving patient quality of life.[2]

Optical imaging is a highly sensitive imaging modality that uses visible light to visualize soft tissues in the body. Traditional optical imaging probes such as fluorescent organic molecules and fluorescent proteins are limited by phenomena such as autofluorescence and photobleaching.[3,4] These limitations render the discrimination between signals due to naturally luminescent biological molecules and the fluorescent probe extremely difficult. In comparison,

lanthanide ions such as Europium (III) exhibit long-lived luminescent lifetimes, allowing for time-resolved luminescent image acquisition.[4] Additionally, Eu(III)-based complexes have the potential for increased depth of tissue penetration, due to their emission of light in the red region of the electromagnetic spectrum. This makes them ideal candidates for optical imaging *in vivo*. Due to the forbidden nature of the *f-f* orbital transitions responsible for their optical properties, Eu(III) complexes exhibit low molar absorptivity coefficients, which necessitates the use of high energy lasers to obtain high resolution images and could potentially be damaging to biological tissue.[6] To overcome this limitation, an organic chromophore can be used as an "antenna" to sensitize the luminescence of the lanthanide ion upon excitation at a lower energy.[7] The intramolecular energy transfer that results in the luminescence sensitization process is commonly referred to as the antenna effect. The efficiency of this sensitization process is influenced by the nature of, and the distance from the lanthanide ion.[5,7] Direct coordination of the antenna to the lanthanide ion is typically more favorable for the sensitization process, due to a shorter distance, while the possession of an optimal triplet excited state energy maximizes energy transfer to the Ln(III) excited state, while preventing back energy transfer.[5]

Previous studies have shown that quinoline chromophores exhibit triplet state energies similar to that of Eu(III) ions.[5] Based on these results, we sought to further investigate how minor variations in the quinoline structure influence the sensitization efficiency of the antenna. The specific goal of this project was to evaluate the effect of varying the position of a coordinating amide substituent on the optical imaging properties of Eu(III) complexes containing an appended quinoline antenna. The incorporation of the quinoline substituent through an amide functional group serves as a means to stabilize the resulting metal complex, through coordination between the "hard" oxygen atom and the "hard" Eu(III) ion. A library of Europium (III) complexes were synthesized and their luminescent properties have been studied (Figure 1). The central hypothesis of this project was that the position of the amide substituent on the quinoline antenna would alter its electronic properties and this would be reflected in the luminescence intensities of the Eu(III) complexes.

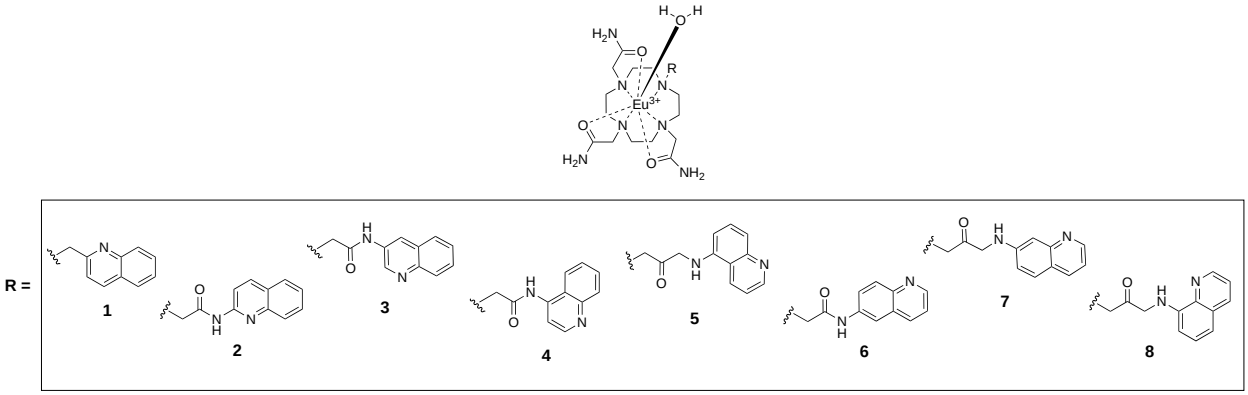

Figure 1. Structures of library of Europium (III) complexes.

2. Methods

2.1 Chemicals and Materials

All reagents and solvents were purchased from commercial sources and used as received. Distilled water was used in all reactions. ^{1}H and ^{13}C NMR spectra were recorded on a Varian 500 MHz NMR spectrometer. Inductively Coupled Plasma was performed using a Perkin Elmer 5300 DV optical emission ICP. High performance liquid chromatography (HPLC) was performed using an Agilent 1100 Series HPLC. UV-Vis absorption spectra were acquired using a Cary 5000 UV-Vis-NIR spectrophotometer. Luminescence studies were performed using a Jobin-Yvon Horiba Fluoromax spectrometer.

2.2 Synthesis and Purification

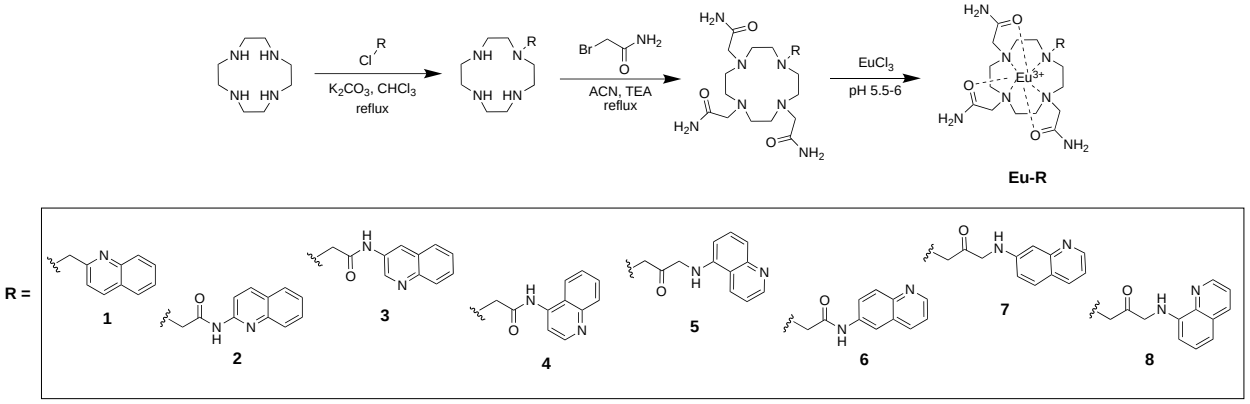

Scheme 1. General synthetic scheme of the library of complexes used in this study.

2.3 General Monoalkylation Synthetic Procedure

Quinoline chloroacetamide sidearms were prepared using previously established procedures.[8] Cyclen (4 equiv) was reacted with the corresponding quinoline sidearm (1 equiv) in the presence of K_2CO_3 (1.2 equiv) in chloroform (25 mL). The mixture was stirred to reflux overnight. The reaction mixture was washed with water (1 x 40 mL) and extracted with HCl (0.3 M x 25 mL). The aqueous layer was recovered, and the pH adjusted to pH 8. The layer was then extracted with $CHCl_3$ (3 x 25 mL). The pH was further adjusted to pH 11 and extracted with $CHCl_3$ (6 x 25 mL). The solution was dried with Na_2SO_4, filtered, and the solvent removed under reduced pressure, to yield the desired products in 69 % - 96% yields.

2.4 General Trialkylation Synthetic Procedure

The monoalkylated cyclen compounds (1 equiv) were reacted with 2-bromoacetamide (3.1 equiv) in the presence of triethylamine (4 equiv) in acetonitrile (20 mL). The mixture was stirred to reflux overnight. The reaction mixture was vacuum filtered, and the residue washed multiple times with cold acetonitrile, to yield the final solid products in 35 % - 73 % yields.

2.5 General Metal Complexation Procedure

Each ligand was dissolved in H_2O (7 mL) and the pH of the solution adjusted to pH 6 using 0.3 M HCl. An equimolar amount of aqueous $EuCl_3$ was added, and the solution was stirred at room temperature overnight. The pH was raised to pH 10 by addition of 0.3 NaOH to precipitate excess Eu^{3+}as $Eu(OH)_3$. The precipitate was removed by syringe filtration, and the absence of free metal was confirmed using a Xylenol Orange test. The pH of the solution was adjusted to 7 and lyophilized to yield all the Eu(III) complexes used in this study as solids. HPLC and Mass Spectrometry were used to verify the purity and identity of the metal complexes.

2.6 ^{1}H and ^{13}C NMR data for Ligands 1 – 8

2.6.1 2-[4,7-bis(carbamoylmethyl)-10-[(quinolin-2-yl)methyl]-1,4,7,10 tetraazacyclododecan-1-yl]acetamide

(1): white solid (0.449 g, 77%). **^{1}H NMR** (D_2O, 500 MHz): δ 2.28-2.43 (m, 16H, N$\underline{CH_2CH_2}$N), 2.71 (s, 4H, N$\underline{CH_2}$C=O), 2.87-2.91 (m, 2H, N$\underline{CH_2}$C=O), 3.34 (s, 2H, N$\underline{CH_2}$-quin), 7.12-7.14 (d, 1H, *J* = 10 MHz, quin-H3), 7.35-7.38 (m, 1H, quin-H6), 7.33-7.56 (m, 1H, quin-H7), 7.64-7.66 (d, 1H, *J* = 10 MHz, quin-H8), 7.73-7.75 (d, 1H, *J*= 10

MHz, quin-H5), 7.96-7.98 (d, 1H, *J*= 10 MHz, quin-H4). **^{13}C NMR** (D_2O, 125 MHz): δ 51.90, 52.27, 52.50, 56.97, 57.02, 57.15, 61.09, 121.67, 126.85, 126.99, 127.11, 127.98, 130.35, 137.64, 146.11, 158.66, 177.12, 177.29

2.6.2 N-(quinolin-2-yl)-2-[4,7,10-tris(carbamoylmethyl)-1,4,7,10-tetraazacyclododecan-1-yl]acetamide

(2). white solid (0.170 g, 35 %). **^{1}H NMR** (D_2O, 500 MHz): δ 2.89-3.48 (m, 18H, N$\underline{CH_2CH_2}$N$\underline{CH_2}$C=O), 3.84 (s, 2H, N$\underline{CH_2}$C-quin), 4.06-4.15 (q, 4H, *J* = 10 MHz, N$\underline{CH_2}$C=O), 7.34-7.36 (d, 1H, *J* = 10 MHz, quin-H6), 7.68-7.70 (td, 1H, *J* = 5 MHz, quin-H7), 7.90-7.94 (m, 2H, quin-8 and quin-3), 8.00-8.01 (d, 1H, *J* = 5 MHz, quin-H5), 8.73-8.75 (d, 1H, *J* = 10 MHz, quin-H4) **^{13}C NMR** (D_2O, 125 MHz): δ 48.15, 51.72, 53.53, 54.68, 113.35, 119.28, 124.85, 128.62, 129.05, 134.19, 134.80, 147.67, 148.57, 167.90, 174.38

2.6.3 N-(quinolin-3-yl)-2-[4,7,10-tris(carbamoylmethyl)-1,4,7,10-tetraazacyclododecan-1-yl]acetamide

(3): tan solid (0.349 g, 54 %). **^{1}H NMR** (D_2O, 500 MHz): δ 2.86-3.59 (m, 22H, N$\underline{CH_2CH_2}$Nand $\underline{CH_2CH_2}$C=O), 4.00 (s br, 2H, N$\underline{CH_2}$C-quin), 7.50-7.53 (m, 1H, quin-H6), 7.62-7.65 (m, 1H, quin-H7), 7.69-7.71 (d, 1H, *J* = 10 MHz, quin-H5), 7.76-7.77 (d, 1H, *J* = 5 MHz, quin-H8), 8.32 (s br, 1H, quin-H4), 8.67-8.68 (d, 1H, *J* = 5 MHz, quin-H2) **^{13}C NMR** (D_2O, 125 MHz): δ 48.45, 51.42, 54.35, 54.55, 54.98, 57.36, 124.84, 127.81, 127.93, 128.06, 128.42 130.56, 131.52, 140.54, 141.89, 167.33, 168.00

2.6.4 N-(quinolin-4-yl)-2-[4,7,10-tris(carbamoylmethyl)-1,4,7,10-tetraazacyclododecan-1-yl]acetamide

(4): white solid (0.408 g, 72 %). **^{1}H NMR** (D_2O, 500 MHz): δ 2.90-3.12 (m, 18H, N$\underline{CH_2CH_2}$N$\underline{CH_2}$C=O), 3.87 (s br, 2H, N$\underline{CH_2}$C-quin), 4.09 (s br, 4H, N$\underline{CH_2}$C=O), 7.57-7.60 (m, 1H, quin-H3), 7.83-7.86 (m, 1H, quin-H7), 7.92-7.93 (d, 1H, *J* = 5 MHz, quin-H6), 8.04-8.05 (d, 1H, *J* = 5 MHz, quin-H8), 8.21-8.22 (d, 1H, *J* = 5 MHz, quin-H5), 8.56-8.57 (d, 1H, *J* = 5 MHz, quin-H2). **^{13}C NMR** (D_2O, 125 MHz): δ 48.33, 51.64, 54.27, 54.58, 55.50, 57.36, 110.43, 119.51, 122.04, 122.14, 128.72, 133.87, 139.99, 145.36, 147.81, 168.19, 172.42

2.6.5 N-(quinolin-5-yl)-2-[4,7,10-tris(carbamoylmethyl)-1,4,7,10-tetraazacyclododecan-1-yl]acetamide

(5): golden yellow solid (0.474 g, 66 %). **^{1}H NMR** (D_2O, 500 MHz): δ 2.46-2.63 (m, 16H, N$\underline{CH_2CH_2}$N), 2.90-2.93 (d, 6H, *J* = 15 MHz, N$\underline{CH_2}$C=O), 3.24 (s, 2H, N$\underline{CH_2}$C-quin), 7.36-7.38 (m, 2H, quin-H3 and H6), 7.60-7.63 (m, 1H, quin-H7), 7.80-7.81 (d, 1H, *J* = 5 MHz, quin-H8), 8.04-8.06 (d, 1H, *J* = 10 MHz, quin-H4), 8.67 (s, 1H, quin-H2). **^{13}C NMR** (D_2O, 125 MHz): δ 52.24, 52.43, 56.87, 57.14, 57.33, 58.17, 121.79, 124.22, 124.52, 124.58, 127.17, 129.74, 131.80, 132.18, 146.97, 147.00, 150.47, 173.64, 176.78

2.6.6 N-(quinolin-6-yl)-2-[4,7,10-tris(carbamoylmethyl)-1,4,7,10-tetraazacyclododecan-1-yl]acetamide

(6): tan solid (0.427 g, 65 %). **^{1}H NMR** (D_2O, 500 MHz): δ 2.93-3.50 (m br, 18H, N$\underline{CH_2CH_2}$N$\underline{CH_2}$C=O), 3.66 (s br, 2H, N$\underline{CH_2}$C-quin), 4.06 (s br, 4H, N$\underline{CH_2}$C=O), 7.86-7.89 (m, 1H, quin-H3), 7.94 (s br, 1H, quin-H7), 8.01 (s br, 1H, quin-H5), 8.32 (s br, 1H, quin-H8), 8.80 (s br, 1H, quin-H4), 8.85-8.86 (d, 1H, *J* = 5 MHz, quin-H2). **^{13}C NMR** (D_2O, 125 MHz): δ 48.47, 51.46, 54.52, 54.71, 55.26, 57.35, 110.12, 116.52, 121.01, 122.04, 128.83, 129.60, 134.38, 138.36, 142.63, 146.64, 167.46

2.6.7 N-(quinolin-7-yl)-2-[4,7,10-tris(carbamoylmethyl)-1,4,7,10-tetraazacyclododecan-1-yl]acetamide

(7): orange solid (0.4786 g, 56 %). **^{1}H NMR** (D_2O, 500 MHz): δ 2.86-3.62 (m, 22H, N$\underline{CH_2CH_2}$N$\underline{CH_2}$C=O), 4.02 (s br, 2H, N$\underline{CH_2}$C-quin), 7.60-7.62 (d, 1H, *J* = 10 MHz, quin-H3), 7.72-7.74 (t, 1H, *J*= 5 MHz, quin-H6), 7.99-8.01 (d,

1H, *J* = 10 MHz, quin-H8), 8.37 (s, 1H, quin-H4), 8.79-8.81 (d, 2H, *J* = 10 MHz, quin-H5 and quin-H2). **^{13}C NMR** (D_2O, 125 MHz): δ 48.51, 51.46, 54.51, 54.84, 55.30, 57.34, 106.86, 120.07, 123.47, 126.01, 130.16, 138.58, 143.24, 143.71, 146.71, 167.95, 171.67

2.6.8 N-(quinolin-8-yl)-2-[4,7,10-tris(carbamoylmethyl)-1,4,7,10-tetraazacyclododecan-1-yl]acetamide

(8): white solid (0.375 g, 73%). **^{1}H NMR** (D_2O, 500 MHz): δ 3.14-3.32 (m br, 18H, $NCH_2CH_2NCH_2C$=O), 3.87 (s br, 6H, NCH_2C-quin), 7.48 (s br, 2H, quin-H7 and quin-H3), 7.65 (s br, 1H, quin-H5), 8.05-8.06 (d, 1H, *J* = 5 MHz, quin-H6), 8.26 (s br, 1H, quin-H4), 8.70 (s, 1H, quin-H2).**^{13}C NMR** (D_2O, 125 MHz): δ 49.32, 50.70, 54.46, 54.99, 55.09, 57.36, 122.07, 122.30, 125.35, 126.98, 128.48, 131.74, 138.52, 138.77, 149.23 167.26, 169.29

2.7 Absorption and Luminescence Measurements

Solutions of each Eu(III) complex were prepared at 0.05 mM (absorption measurements) and 0.1 mM (emission and excitation measurements) in 0.1 mM HEPES buffer (pH 7.4). Absorbance spectra were acquired over a 200-800 nm range at room temperature using a 1.0 cm quartz cuvette and 5 nm slit width. Excitation spectra were acquired from 200-450 nm with an emission monochromator slit width of 2 nm. Emission spectra were collected from 550-750 nm with an excitation monochromator slit width of 2 nm. All spectra were acquired at room temperature using a 1.0 cm quartz cuvette. A 450 nm long pass filter was used to eliminate second order peaks.

2.8 Lifetime Measurements

Phosphorescent decay by delay measurements were acquired using a flash count of 50, sample window of 0.2 ms, 0.05 ms delay increment, 5 ms max delay, and an initial delay of 0.05 ms. Samples were prepared by lyophilizing aliquots of each lanthanide solution in 500 mL of 0.1 mM HEPES buffer (pH 7.4). One aliquot of each lanthanide solution was then redissolved in D_2O and lyophilized. These samples were dissolved once more in D_2O and lyophilized. Solutions at 0.02 mM concentration were made by dissolving the compounds in HEPES buffer or D_2O. The data was fit with a mono-exponential decay function to obtain τ values. The number of bound water molecules (q) was determined using equation 1 where *x* represents the number of amide protons in each complex.[9]

$$q = 1.2[(k_{H_2O} - k_{D_2O}) - 0.25 - 0.075x] \quad \textbf{(1)}$$

3. Results

To assess the luminescence sensitization of the Eu(III) complexes by the quinoline moiety, excitation and emission spectra were acquired. Excitation spectra are typically used to evaluate the amount of energy required to excite an electron from the singlet ground state to the singlet excited state of the chromophore. A fluorescent probe is most efficiently excited by light of a particular wavelength, referred to as the λ_{max} of excitation. The intensity of the emitted light is maximized for a particular fluorescent probe when excited at this specific wavelength.[10] As demonstrated in Figure 2, luminescence sensitization via excitation of the quinoline antenna was achieved for the library of Eu(III) complexes. Peak shoulders and secondary peaks were observed in all recorded spectra and these were attributed to the complexes possessing multiple energy levels of similar energies in the excited states.[11] All of the complexes possess a similar λ_{max} of excitation, between 315 and 330 nm, which correlate to the $\pi \rightarrow \pi^*$ electronic transitions of the quinoline antenna; however; the λ_{max} of Eu-44 is considerably right-shifted to 354 nm (Figure 2). This observed difference is possibly due to increased conjugation of the quinoline brought about by the presence of the amide-substituent in a *para*- position relative to the nitrogen in the quinoline moiety.

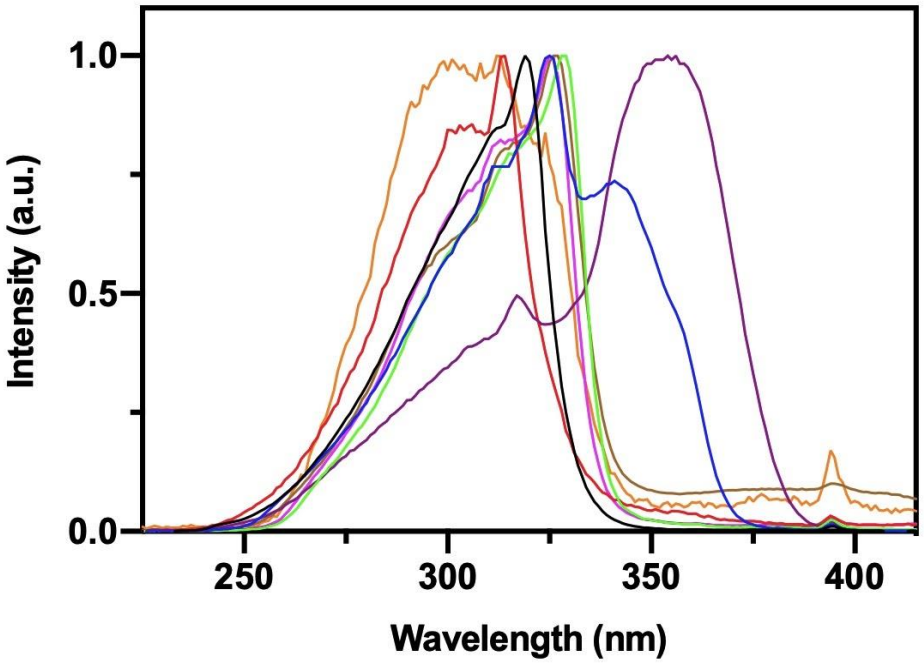

Figure 2. Normalized excitation spectra of all complexes prepared at 0.1 mM with 0.1 mM HEPES buffer (pH 7.4). Spectra were acquired at room temperature from 200-450 nm with an emission monochromator slit width of 2 nm. Eu-1 (black), Eu-2 (blue), Eu-3 (green), Eu-4 (purple), Eu-5 (red), Eu-6 (pink), Eu-7 (brown), Eu-8 (orange).

Emission spectra of Europium (III) complexes provide important insight about the luminescence and structural properties of the compounds.[12,13] A general Eu(III) spectrum consists of seven key electronic transitions. The key peaks include the $^5D_0 \rightarrow {}^7F_0$ transition which occurs between 570-585 nm. Observation of this peak corresponds to the symmetry of the molecule. The $^5D_0 \rightarrow {}^7F_1$ transition occurring between 585-600 nm is the magnetic dipole transition that is independent of the Eu^{3+} environment. Its intensity is used to normalize and compare luminescence intensities between different Eu(III) complexes. The $^5D_0 \rightarrow {}^7F_2$ transition that occurs between 610-630 nm is the hypersensitive transition, meaning its intensity is influenced by the local symmetry of the Eu(III) ion.[12] This transition is responsible for the red luminescence color that is observed. The $^5D_0 \rightarrow {}^7F_3$ transition occurs between 640-660 nm and is generally very weak because it is forbidden by the Judd-Ofelt theory.[12,13] This transition is due to J-mixing and is not considered when the Eu(III) complex is used for optical imaging.[12] The $^5D_0 \rightarrow {}^7F_4$ transition occurs between 680-710 nm and its intensity is dependent on the chemical environment, however, it is not hypersensitive like the $\Delta J = 2$ peak.[12] This peak is generally interpreted through comparison to the $\Delta J = 1$ peak as the $\Delta J = 4$ transition lies in the spectral region where most photomultiplier tubes have low sensitivity. The $^5D_0 \rightarrow {}^7F_5$ and $^5D_0 \rightarrow {}^7F_6$ transitions, occurring between 740-770 nm and 810-810 nm, respectively, are not typically discussed as many spectrofluorometers have very low spectral sensitivity in the region where these peaks occur.[12] As observed in Figure 3, all of the complexes in this library exhibit the same general Eu(III) emission profile which confirms that the observed luminescence of each complex is attributed to the presence of the Eu(III) ion. The intensity differences can be attributed to variations in the photophysical properties of these complexes caused by changing the position of the coordinating amide substituents on the quinoline moiety.

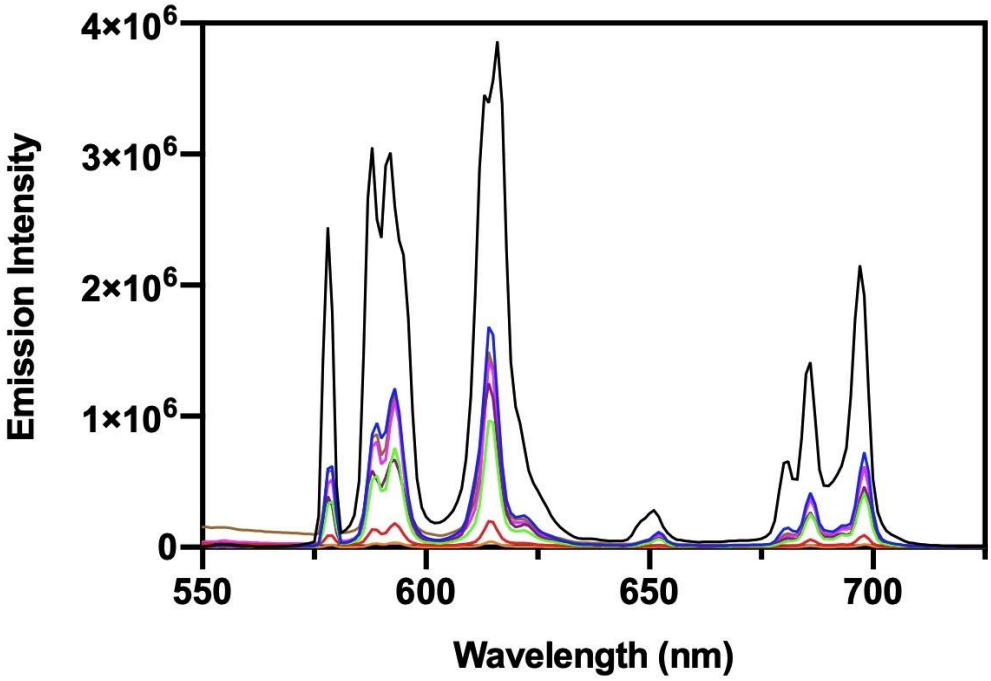

Figure 3. Emission spectra of 0.1 mM complexes prepared in 0.1 mM HEPES buffer (pH 7.4). Spectra were acquired at room temperature from 570-750 nm with an excitation monochromator slit width of 2 nm. Eu-1 (black), Eu-2 (blue), Eu-3 (green), Eu-4 (purple), Eu-5 (red), Eu-6 (pink), Eu-7 (brown), Eu-8 (orange).

Eu-1 exhibited the largest emission intensity of all the complexes in this study due to the direct coordination, and therefore shorter distance, of the quinoline pendant arm to the Eu(III) ion (Figure 3).[1] For all other complexes in this study, a clear trend between the position of the amide substituent and magnitude of emission intensity was not observed. For example, Eu-7 and Eu-6, which have the amide substituent on the benzene ring of the quinoline had the third and fourth largest emission profiles, respectively. However, Eu-5 and Eu-8, which also contained a benzene substituted amide exhibited the lowest emission intensities. For complexes Eu-5 and Eu-8, we suspect that these very low emission intensities are most likely due to a poor match between the triplet state energies of the antenna and the Eu(III) in these complexes.

In order to confirm that the observed luminescence was due to the intramolecular energy transfer via the quinoline antenna, the emission spectra of each complex was acquired upon direct excitation of the Eu(III) ion at 395 nm and compared to the results obtained upon excitation of the chromophore. As indicated in Figure 4, the luminescence intensities are far greater when the quinoline is excited in comparison to direct excitation of the metal ion. This indicates that the quinoline is effectively sensitizing the luminescence of the europium ion in each of the complexes regardless of the identity of the quinoline amide side-chain.

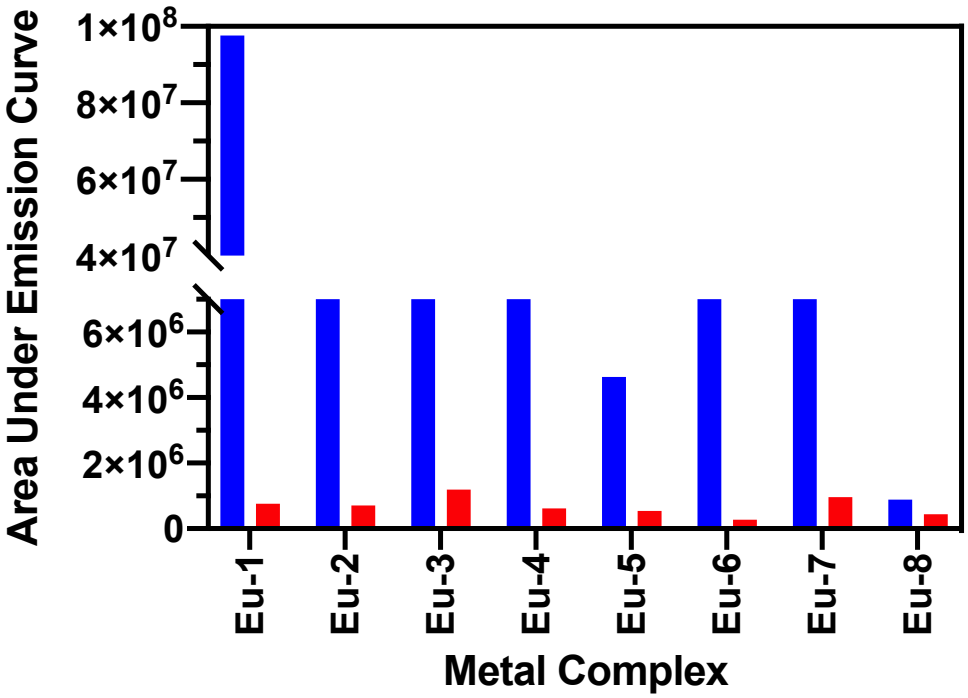

Figure 4. Comparison of areas under the emission spectra upon excitation of the quinoline antenna (blue) and direct excitation of the lanthanide ion at λ_{ex} = 395 nm (red).

The long-lived luminescent lifetimes of lanthanide ions can be used to approximate the number of bound water molecules on the Ln(III) ion. The lifetimes of Eu(III) complexes are measured via phosphorescence decay by delay in which the observed lifetime in D_2O is expected to be roughly double the lifetime in HEPES buffer (H_2O). This relationship is expected because the vibrational frequencies of the O-H bonds in water are similar to those of Eu(III); therefore they will induce quenching of the luminescence.[15,16] The results of the experimental luminescent lifetimes of the complexes measured in D_2O and H_2O are summarized in Table 1. With the exception of Eu-5, all complexes were found to exhibit a lifetime in D_2O that was at least twice the magnitude of the lifetime in H_2O (Figure 5, Table 1). One possible explanation for this observation is that Eu-5 complex may possess energy levels through which the decay of emission proceeds by vibrational relaxation, even in D_2O.[14] This hypothesis is supported by the relatively low emission intensity of Eu-5 compared to the other complexes in this study. The number of bound water molecules for each complex (q value) was calculated using Equation (1). Amide protons were included in the q value calculation because, similar to O-H oscillators, N-H oscillators have also been found to quench Eu(III) emission.[15] Every complex in this study was found to possess approximately one bound water molecule with the exception of Eu-5. This is for the most part consistent with the fact that the Eu(III) ion has nine coordination sites, and is chelated by octadentate ligands, thus leaving one coordination site available for a water molecule to bind.[7] It is also important to note that this approach to estimating q-values is known to have an error of ± 0.5 in some cases, and may also explain the low q-value for Eu-5.[9] The presence of a single bound water molecule is critical for these complexes to serve as dual-modality imaging agents for both optical and PARACEST MR imaging modalities; however, bound water molecules also reduce the quantum yields of these complexes due to their emission quenching effects. Nevertheless, our primary aim was to identify the metal complex that possessed the optimal combination of quantum yield and kinetic stability in spite of the presence of this bound water molecule.

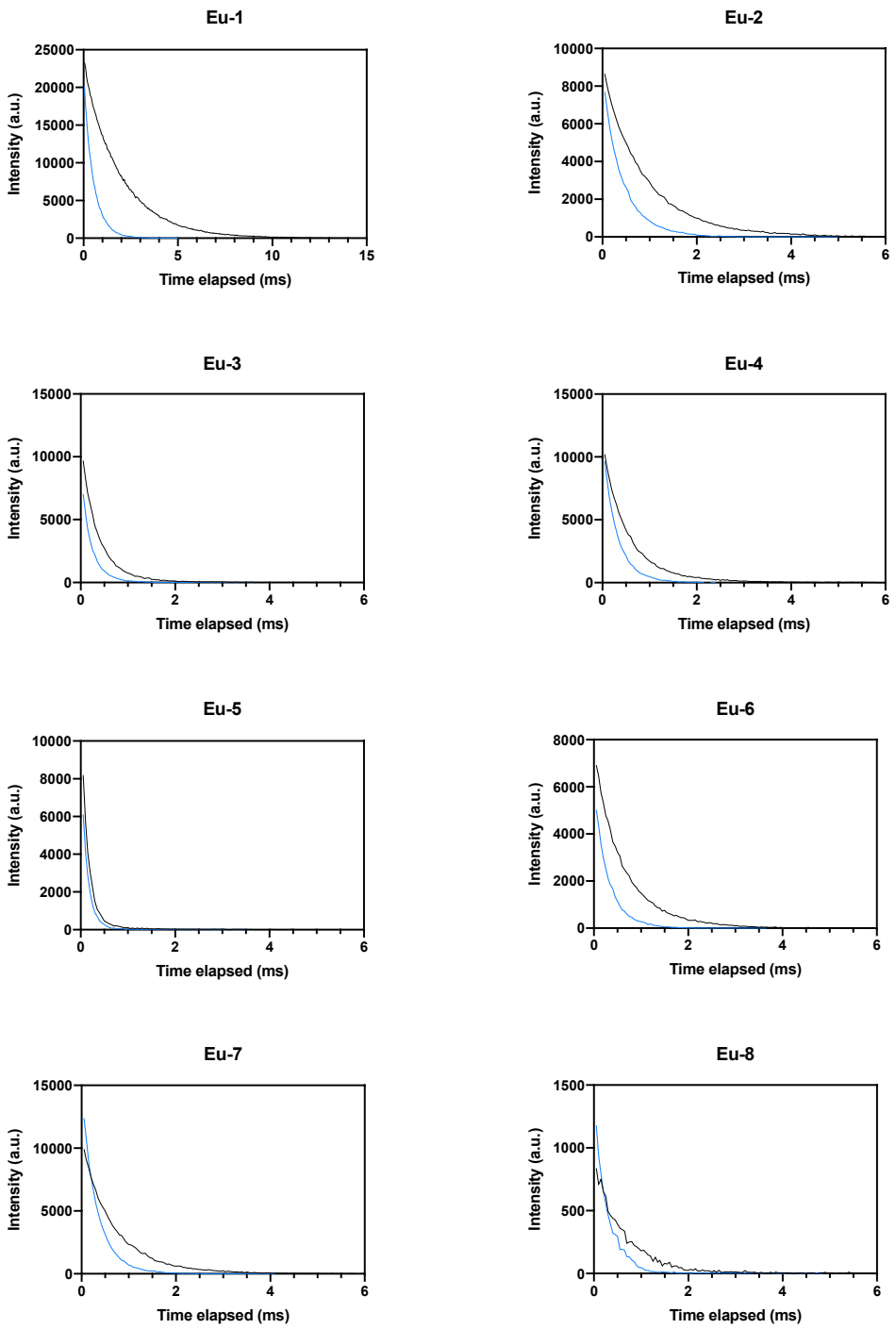

Figure 5. Luminescence lifetimes of 0.1 mM complexes in 0.1 mM HEPES buffer (pH 7.4) (blue) and D_2O (black) acquired via phosphorescence decay by delay measurements using a flash count of 50, sample window of 0.2 ms, 0.05 ms delay increment, 5 ms max delay, and an initial delay of 0.05 ms

Table 1. Lifetime measurements and q values of 0.1 mM complexes in 0.1 mM HEPES buffer (pH 7.4) and D_2O.

Compound	τ D_2O (ms)	τ H_2O (ms)	k D_2O (ms^{-1})	k H_2O (ms^{-1})	q value[a]
Eu-1	1.93	0.504	0.519	1.98	0.916
Eu-2	0.893	0.417	1.12	2.40	0.602
Eu-3	0.358	0.213	2.79	4.69	1.35
Eu-4	0.532	0.293	1.88	3.42	0.915
Eu-5	0.152	0.133	6.57	7.55	0.239
Eu-6	0.623	0.301	1.61	3.32	1.12
Eu-7	0.682	0.325	1.47	3.08	1.00
Eu-8	0.611	0.292	1.64	3.42	1.21

[a]The number of bound water molecules, q, was calculated using the equation $q = 1.2[(k_{H_2O} - k_{D_2O}) - 0.25 - 0.075x]$ where x is the number of amide protons in each complex.

4. Conclusion

In this project, we found that the appended quinoline antenna sensitizes the luminescence capabilities of this library of Eu(III) complexes however, the efficiency of the sensitization process is significantly influenced by the location of the amide substituent on the quinoline pendant arm. Eu-1, Eu-3, Eu-6, and Eu-7 exhibited the highest emission intensities while Eu-5 and Eu-8 exhibited the lowest emission intensities upon excitation of the quinoline antenna. Although Eu-1 was found to exhibit the highest emission intensity due to the shorter distance between the sensitizer and the Eu(III) ion, we anticipate that this complex would exhibit poor kinetic stability compared to the others due to the absence of the additional coordinating amide oxygen. The majority of the complexes also appeared to possess one Eu(III) bound water molecule, the exchange of which could potentially serve as a source of MRI contrast. Future work includes investigation of the stabilities of these complexes at physiological temperatures and evaluation of their MRI properties.

5. Acknowledgements

The authors would like to acknowledge funding from the USF Faculty Development Fund (FDF) and the USF Startup Funds. We would also like to extend our appreciation to the Faculty and Staff in the Chemistry Department at USF for their support and guidance. Finally, we want to acknowledge the members of the Evbuomwan lab: Matthew Derfus, Holly Clancy, and Megan Martin for their scientific discussions and moral support.

6. References

1. Heffern, M. C.; Matosziuk, L. M.; Meade, T. J. Lanthanide Probes for Bioresponsive Imaging. *Chem. Rev*. **2014**, 114 (8), 4496–4539.

2. Bu, Lihong; Shen, Baozhong; Cheng, Z. Fluorescent Imaging of Cancerous Tissues for Targeted Surgery. *Adv. Drug Deliv. Rev*. **2014**, 76 (21).

3. Rich, R. M.; Stankowska, D. L.; Maliwal, B. P.; Sørensen, T. J.; Laursen, B. W.; Krishnamoorthy, R. R.; Gryczynski, Z.; Borejdo, J.; Gryczynski, I.; Fudala, R. Elimination of Autofluorescence Background from Fluorescence Tissue Images by Use of Time-Gated Detection and the AzaDiOxaTriAngulenium (ADOTA) Fluorophore. *Anal. Bioanal. Chem*. **2013**, 405 (6), 2065–2075.

4. Wei, L.; Yan, W.; Ho, D. Recent Advances in Fluorescence Lifetime Analytical Microsystems: Contact Optics and CMOS Time-Resolved Electronics. *Sensors (Switzerland)* **2017**, 17 (12).

5. Mihorianu, M.; Leonzio, M.; Monari, M.; Ravotto, L.; Ceroni, P.; Bettinelli, M.; Piccinelli, F. Structural and Spectroscopic Properties of New Chiral Quinoline-Based Ln(III) Complexes. *ChemistrySelect* **2016**, 1 (9), 1996–2003.

6. James, M. L.; Gambhir, S. S. A Molecular Imaging Primer: Modalities, Imaging Agents, and Applications. *Physiol. Rev.* **2012**, 92 (2), 897–965.

7. Hammoud, H.; de Bettencourt-Dias, A.; Schmitt, M.; Monteiro, J. H. S. K.; Rossini, J. S.; Lecointre, A.; Gallet, S.; Bourguignon, J. J.; Mameri, S. Unusual O-Bridged Symmetric Quinoline-Based Ligand for the Formation of Luminescent Mono-Aqua Lanthanide Complexes. *ChemistrySelect* **2016**, 1 (21), 6618–6622.

8. Evbuomwan, O. M.; Kiefer, G.; Sherry, A. D. Amphiphilic EuDOTA-Tetraamide Complexes Form Micelles with Enhanced CEST Sensitivity. *Eur. J. Inorg. Chem.* **2012**, 2126–2134.

9. Beeby, A.; Clarkson, I. M.; Dickins, R. S.; Faulkner, S.; Parker, D.; Royle, L.; deSousa, A. S.; Williams, J. A. G.; Woods, M. Non-Radiative Deactivation of the Excited States of Europium, Terbium and Ytterbium Complexes by Proximate Energy-Matched OH, NH and CH Oscillators: An Improved Luminescence Method for Establishing Solution Hydration States. *J. Chem. Soc. Perkin Trans*. 2, **1999**, 2(3), 493–504

10. M. Sauer, J. Hofkens, J. Enderlein. Handbook of Fluorescence Spectroscopy and Imaging; Wiley-VCH: Weinheim, Germany, 2011, pp. 43-47

11. Albani, J. R. Fluorescence: Principles and Observables. In *Structure and Dynamics of Macromolecules: Absorption and Fluorescence Studies*; **2004**, 55-98.

12. K. Binnemans, Interpretation of europium (III) spectra. *Coord. Chem. Rev.* **2015**, 295, 1–45.

13. Lowther, J. E. Spectroscopic Transition Probabilities of Rare Earth Ions. *J. Phys. C Solid State Phys.* **1974**, *7* (23), 4393–4402.

14. Hasegawa, Y.; Wada, Y.; Yanagida, S. Strategies for the Design of Luminescent Lanthanide(III) Complexes and Their Photonic Applications. *J. Photochem. Photobiol. C Photochem. Rev*. **2004**, 5 (3), 183–202.

15. Ilichev, V. A.; Silantyeva, L. I.; Kukinov, A. A.; Bochkarev, M. N. Photophysical Properties of IR Luminescent Lanthanide Complexes with Polyfluorinated Ligands. *Ineos Open* **2019**, 2 (3).

16. Khullar, S.; Singh, S.; Das, P.; Mandal, S. K. Luminescent Lanthanide-Based Probes for the Detection of Nitroaromatic Compounds in Water. *ACS Omega* **2019**, 4 (3), 5283–5292.